F. W. Klaiber, R. A. Lohnes, L. W. Zachary, T. A. Austin,
B. T. Havens, B. T. McCurnin

Design Methodology for Corrugated Metal Pipe Tiedowns: Phase I

February 1993

**Iowa Department
of Transportation**

report College of
Engineering
Iowa State University

F. W. Klaiber, R. A. Lohnes, L. W. Zachary, T. A. Austin,
B. T. Havens, B. T. McCurnin

Design Methodology for Corrugated Metal Pipe Tiedowns: Phase I

engineering research institute

iowa state university

ABSTRACT

Questionnaires were sent to transportation agencies in all 50 states in the U.S., to Puerto Rico, and all provinces in Canada asking about their experiences with uplift problems of corrugated metal pipe (CMP). Responses were received from 52 agencies who reported 9 failures within the last 5 years. Some agencies also provided design standards for tiedowns to resist uplift. There was a wide variety in restraining forces used; for example for a pipe 6 feet in diameter, the resisting force ranged from 10 kips to 66 kips. These responses verified the earlier conclusion based on responses from Iowa county engineers that a potential uplift danger exists when end restraint is not provided for CMP and that existing designs have an unclear theoretical or experimental basis.

In an effort to develop more rational design standards, the longitudinal stiffness of three CMP ranging from 4 to 8 feet in diameter were measured in the laboratory. Because only three tests were conducted, a theoretical model to evaluate the stiffness of pipes of a variety of gages and corrugation geometries was also developed. The experimental results indicated a "stiffness" EI in the range of 9.11×10^5 k-in^2 to 34.43×10^5 k-in^2 for the three pipes with the larger diameter pipes having greater stiffness. The theoretical model developed conservatively estimates these stiffnesses.

Recognizing that soil over and around CMP's will contribute to their stiffness, one field test was conducted on a pipe 10

feet in diameter. The test was conducted with 2 feet of soil cover and a foreslope of 2:1. This test indicated that the soil cover significantly increased the stiffness of the pipe.

Future plans include development of a finite element analysis to better describe the soil structure interaction. With those relationships and the data from additional field tests, design standards based on a rational design procedure will be developed. The soil-structure analysis and the development of design standards for CMP tiedowns will comprise the final phase of this study.

v

TABLE OF CONTENTS

LIST OF TABLES

LIST OF FIGURES

1. THE PROBLEM AND OBJECTIVES

1.1. The Problem

In the mid 1970's Iowa Department of Transportation (Iowa DOT) and Federal Highway Administration (FHWA) recognized that corrugated metal pipe (CMP) were experiencing an unsuitable number of uplift failures. Iowa DOT and FHWA recommended that, for pipes over 4 ft in diameter, provision should be made for tiedowns at inlets. In spite of these warnings, uplift failures continued to occur; and in 1988, a survey of Iowa county engineers revealed 12% of the 68 counties that responded experienced uplift failures of CMP (Austin et al, 1990). Although this frequency of failure is down from the 16% reported in a 1975 Iowa DOT survey, the number of failures still is unacceptably high.

1.2. Objectives

The goal of this research is to develop a rational method for the design of tiedowns for CMP and to provide standard designs. Because of the formidable scope of this project, the study is divided into two phases with specific objectives in each phase. The objectives of Phase 1 are: a) synthesize design standards from state DOTs around the nation, b) determine longitudinal stiffness of corrugated metal pipe and c) begin to obtain experimental data on soil-CMP interaction. This report addresses the objectives of Phase 1.

The objectives of Phase 2 are: a) Complete collection of data on soil-structure interaction, b) incorporate the water depth computations of Austin et al (1990) into an integrated

program, c) synthesize all of the data into a rational design
procedure and develop software for use on microcomputers and d)
develop design standards for corrugated metal pipe tiedowns.
These objectives will be addressed at a later date.

2. LITERATURE REVIEW

2.1. Types of CMP

Different methods used to fabricate CMP result in four types of pipe. Helical pipes with mechanical seams are corrugated sheets joined with a continuous interlocking helical seam. Helical, welded-seam CMP is similar to helical lock-seam except that the pipe is welded continuously along the helical seam as it is fabricated. Annular pipes with spot-welded seams consist of curved corrugated plates spot-welded to form rings two feet in length. These rings are joined by spot-welds to create CMP of practical lengths. Annular, riveted seam pipes are similar to annular spot-welded except that rivets are used as fasteners instead of welds.

2.2. Potential Failure Modes

There are many possible failure modes for CMP. They are discussed in detail by Watkins (1960) and Kennedy and Laba (1989) and are summarized here:

1) Excessive deflection happens if the foundation soil is highly compressible or the side fill has not been properly compacted as shown in Figure 2.1a.

2) Yielding of the wall section occurs when the soil has considerable passive resistance and the CMP wall thickness is insufficient to resist the superimposed loads. This is shown in Figure 2.1b.

3) Rather than yield in compression, the pipe wall may buckle under high load with inadequate passive resistance from
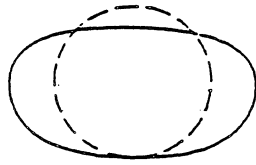
(a)   excessive deflection
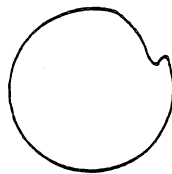
(b)   yielding of the wall section
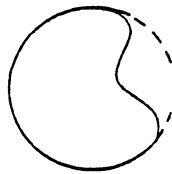
(c)   elastic ring buckling
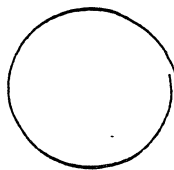
(d)   seam failure

Figure 2.1   Potential failure modes.

the soil. See Figure 2.1c.

4)   Seam failure includes shear of bolts, rivets, or welds at seams and occurs if the pipe is adequate to carry the loads but the fasteners are either substandard or spaced incorrectly. This is illustrated in Figure 2.1d.

5)   Corrosion may create holes which prevent the CMP from remaining watertight.

Longitudinal flexural failure is often overlooked in design and may be as important as consideration of CMP ring bending failure. Possible causes of longitudinal bending, and thus the potential for failure include: pore water uplift below the pipe, differential settlement beneath the pipe, non-uniform bedding support beneath the pipe, frost heave, expansive soils, and earthquakes.

Several uplift failures which were most likely caused by pore water uplift under structural plate culverts are documented by Edgerton (1960) and Austin et al. (1990).

Watkins (1960) discusses the relationship of longitudinal bending stresses which act perpendicular to ring bending stresses in the corrugations. High longitudinal stresses are avoided by the relative compressibility of the corrugations as compared with smooth wall pipe; therefore, biaxial interaction is considered insignificant and longitudinal bending of CMP is analyzed separately from ring bending.

Trautmann et al (1985) employed laboratory test results on scale models to determine the longitudinal force displacement

relationships for the models subjected to vertical ground movement. Kennedy and Laba (1989) discuss lifting of the invert which may be caused by soil settlement under the CMP haunches or from increased water level under the steel structure which creates an uplift on the bottom plates. Moser (1990) quantifies the moment induced in pipes due to settlement and attempts to relate it to deflection of the pipe cross section.

Mayberry and Goodman (1989) discuss a new method of structural plate pipe installation which attempts to minimize the effects of longitudinal bending. The plates are manufactured with yielding seams which are designed to slip during bending and to minimize any potential longitudinal stresses.

Bakht (book in progress) discusses cross-sectional uplift failure of the inlet due to settlement under the haunches and longitudinal uplift failure of the entire pipe end due to bending moments induced by longitudinal settlement and buoyancy effects.

No information was found in the open literature describing methods to estimate the longitudinal strength and stiffness of CMP.

2.3. Design Methods for CMP Subjected to Soil Loads

An equation for estimating the soil load on underground conduits was developed at Iowa State University (Marston, 1930) and as applied to positive projecting conduits (Spangler, 1951)

is:

$$V = \gamma B_c^2 \frac{e^{K\mu'(H/B_c)} - 1}{2K\mu'} \qquad (1)$$

where:

> V = load per longitudinal length of pipe
> H = height of fill above conduit
> γ = unit weight of embankment soil
> K = Rankine's lateral pressure ratio
> μ'= coefficient of friction of fill material
> B_c= outside width of conduit
> e = base of natural logarithms

Spangler (1941) extended Marston's work by developing a method to relate the vertical load on the CMP to the horizontal and vertical deflections. This equation, based on a deflection criterion rather than a strength criterion, follows:

$$\Delta X = D_1 \frac{KVr^3}{EI + 0.061E'r^3} \qquad (2)$$

where:

> ΔX = horizontal deflection of CMP (approximately
>   equal to the vertical deflection)
> K = bedding constant
> V = vertical load per length of pipe
> r = nominal pipe radius
> E = modulus of elasticity of pipe steel
> I = moment of inertia per unit length of cross
>   section of pipe wall
> E'= modulus of soil reaction
> D_1 = deflection lag factor

The deflection lag factor varies from 1 to 2 and is intended to account for yielding of soil on the sides of the CMP which may occur after maximum vertical load has been exerted on the CMP.

Because reverse curvature at the top of the CMP often occurs when vertical deflections exceed 20% of the original vertical diameter (American Iron and Steel Institute, 1967), a factor of safety (FOS) of 4 is applied to this method to limit the deflection to 5% vertically.

White and Layer (1960) describe a design procedure based on the ring compression strength of the pipe wall. This method assumes that the entire prism of soil above the pipe is supported by the walls of the pipe. The relationship is shown as follows:

$$C = P \times \frac{S}{2} \tag{3}$$

where: C = ring compression, lb/ft
        P = soil pressure on top of the pipe, lb/ft^2
        S = span or diameter of pipe, ft

In this method, a FOS of 4 is used to limit the compressive stress in the pipe walls to a hydrostatic soil pressure which is equivalent to the overburden pressure divided by the FOS. No deflection criterion is used.

The ring buckling phenomenon as it pertains to the pipe-soil system has been studied by many researchers (Luscher, 1966; Chelapati and Allgood, 1972; Abdel-Sayed, 1978). A typical buckling

formula developed for CMP is:

$$p* = 1.73\sqrt{\frac{EI\ B\ M_s}{r^3}}$$

(4)

where:

    p* = uniform applied pressure causing elastic
           buckling
    EI = ring bending stiffness of CMP
     B = coefficient of elastic support
    M_s = constrained modulus of soil
     r = nominal radius of tube

Krizek, et al. (1971) found that many of the design methods based on elastic buckling provide similar results except under high fills.

Circumferential loads on the CMP itself are probably highest during the handling and installation process. At that time, the CMP has no support from the lateral resistance of the soil and must depend entirely on the ring bending strength until the CMP is in place, back-filled, and the backfill compacted. With the passage of time, soil arching increases and the vertical load on the pipe decreases. Lefebvre et al. (1976) measured arching effects in an embankment over a large span CMP and concluded that 12 days after construction, the pressure on the pipe was only 25% of the calculated overburden pressure.

2.4. Numerical Analysis Methods for CMP-Soil Interaction

CANDE (Culvert analysis and design) is a finite element computer program developed specifically for the analysis of CMP and soil interaction (Katona et al., 1976). CANDE incorporates

Duncan's constitutive soil model (Duncan et al., 1980). Although advances have been made using finite element modelling for design of CMP installations, the accuracy of modelling is limited primarily by the variations of soil strength and stiffness. Poulos (1974) uses finite difference methods to estimate deflections associated with longitudinal bending.

2.5. Laboratory testing

Laboratory tests of CMP have been conducted by loading pipes to ring failure while attempting to replicate in-situ soil-structure interaction. This includes work done by Meyerhof and Baikie (1963) to evaluate the strength of corrugated sheets under circumferential load which are supported laterally by compacted sand. From these tests, the soil stiffness limit is quantified thus making it possible to determine if the CMP wall will fail by yielding or by elastic buckling. The results of these tests can be combined with the ring compression theory and various buckling theories to form a comprehensive design process.

McVay and Papadopoulos (1986) tested scaled-down pipe-arch models within a soil-filled plexiglass box and measured pore pressures in the back-fill and deflection of the model under loads. Watkins and Spangler (1958) investigated the modulus of passive resistance of the soil and its effect on CMP deflections using similitude techniques. Similitude was also used as a tool to study the effects of loads on underground structures by Young and Murphy (1964) and by Nielson and Statish (1972) and Nielson (1972) to study the soil-culvert system.

Testing to determine CMP longitudinal stiffness was conducted at Ohio State University (Lane, 1965) on 23 specimens including helical lock-seam, annular riveted, and annular spot welded. These tests included pipes up to 3 feet maximum in diameter.

2.6. Field Testing

Full-scale field testing of CMP under soil loads has been performed on a variety of CMP products starting with the tests of Marston and his associates in the 1930's. Those tests validated the theory described in Section 2.3. More recently, Watkins and Moser (1971) describe a testing procedure where loads on the pipes in an embankment are simulated by hydraulic rams which exert a downward force from load beams above the pipe. In other studies, loads on the pipes are exerted by heavily weighted test vehicles with high axle loads (Valentine, 1964; Kay and Flint, 1982; Potter and Ulery, 1989).

Special design considerations are needed for CMP under high fills. This has been studied by Spannagel, et al. (1974) and by Brown, et al. (1968) where various CMP were instrumented and monitored to better understand the effects of large loads on CMP.

Another common field condition arises when culverts under minimum cover (1 to 2 feet in some cases) are not adequately protected from high surface loads. Duncan (1978) analyzed minimum cover situations using finite element analyses to develop a "soil-culvert interaction method" for culvert design. Ahlvin (1960) studied the effects of minimum cover on a small diameter

pipe which was covered with 16 inches of material. Loads on the pipe were created by a vehicle which simulated the axle loads of large aircraft.

2.7. Large Span CMP Considerations

Large diameter CMP require special considerations because of the difficulty in determining the stress distributions around these structures (Selig, 1974). Instrumentation, monitoring, and analysis of these larger structures is detailed by several researchers (Selig et al., 1979; Duncan, 1979; McVay and Selig, 1982; Kay and Flint, 1982).

Longitudinal pipe attachments know as "compaction wings" and "thrust beams" are designed to minimize problems during the pipe installation. These problems may include (Selig et al., 1978): inadequate compaction of soil against the CMP side walls, peaking of the CMP crown and distortion of the shape during backfilling, buckling of the structure from loads imposed by construction equipment, and flattening of the CMP as fill is placed above the crown.

Studies have been conducted to determine the feasibility of using steel-reinforced earth (Kennedy et al., 1988; Kennedy and Laba, 1989) where the reinforcement is placed in horizontal layers throughout the embankment and tied to the pipe to provide support to the CMP.

2.8 Generalizations of Literature Cited

Although considerable attention has been given to the ring strength of CMP and to forces associated with overburden

pressures and live loads, very few studies have addressed

longitudinal stiffness and uplift forces. More specifically,

only the analytical work of Poulos (1974), the model studies of

Trautmann et al (1985), and the laboratory testing of Lane (1965)

provide some insight into the longitudinal response of CMP.

3. SURVEY OF TRANSPORTATION AGENCIES ON CMP TIEDOWNS

3.1 Overview

In order to synthesize design standards for corrugated metal pipe (CMP) culvert inlet restraints used by various transportation agencies, Iowa DOT and ISU sent questionnaires to each of the 50 states, Washington D.C., Puerto Rico and eight provinces of Canada, requesting information on the use of restraints and any uplift problems that may have been encountered in the last five years. The data reported here do not include data for Iowa which are presented elsewhere (Austin et al, 1990).

Fifty two (87%) of 60 agencies responded to the questionnaires. Of those responding, nine agencies report uplift problems in the past five years, and 26 of the 52 regions incorporate some type of an uplift restraint. Eighteen of those 26 agencies developed the restraints in response to earlier problems and twenty-two agencies provided copies of their design standards for end restraints for this survey.

3.2 Summary of Uplift Problems

In lieu of specifically identifying the various transportation authorities that responded, the agencies are identified by number. Table 3.1. summarizes data from seven of the reported uplift problems in some cases incomplete data were available and are indicated by "nd" in the table. Two agencies that experienced uplift problems provided no specific data on the nature of their problems. In all cases, except for Agency 1, the pipes were circular with diameters ranging from 36 to 114 inches.

For the agencies who reported soil cover depths, the cover ranged from 5 to 10 feet with the deepest cover of 10 feet over the largest diameter pipe of 114 inches reported by Agency 6. All problematic pipes were square ended except for Agency 1 with a CMP that had a step beveled inlet and Agency 6 with a beveled inlet on their CMP. In all cases, the damaged pipes were replaced with new CMP and in most situations end restraint was added.

Table 3.1. Summary of CMP Uplift Problems.

Agency	Diameter or span/rise (in.)	Length (ft)	Skew (deg)	Cover depth (ft)
1	180/108	nd	nd	nd
2	72	nd	90	5
	96	nd	90	8
3	60	52	nd	nd
4	36	40	10	"very little"
5	60	nd	nd	5
6	114	164	30	10
7	96	90	0	6

3.3. Types of End Restraints

The variety of end restraints can be classified as anchors, head walls, wing walls, and slope collars. Figure 3.1 shows schematic drawings of each type.

Anchors consist of vertical concrete walls, perpendicular to the axis of the pipe, that extend to mid height of the culvert, and are bolted to the pipe with a large mass of concrete below ground. The pipe ends are beveled above the top of the concrete. In some situations, cutoff walls extend below the concrete anchors.

a) ANCHOR
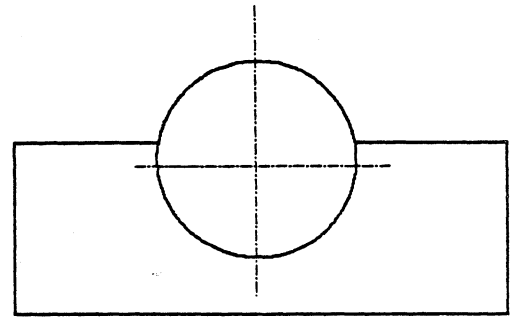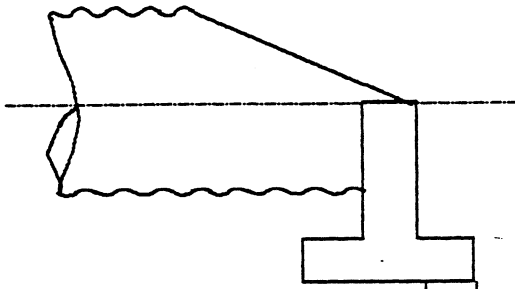
b) FULL STRAIGHT HEADWALL
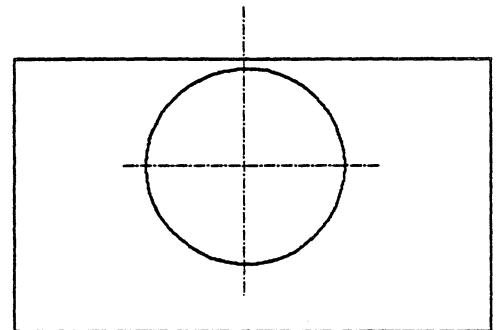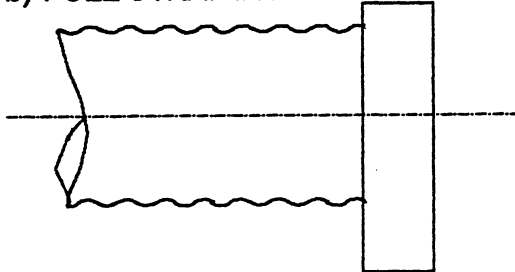
c) WINGWALLS
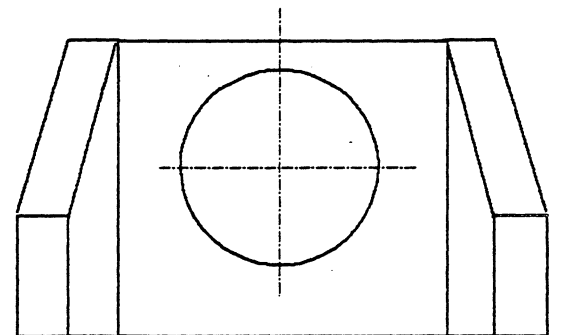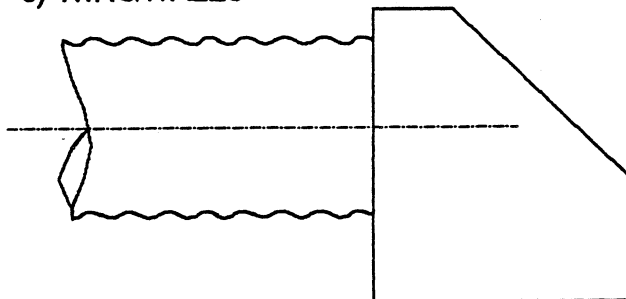
d) SLOPE COLLAR
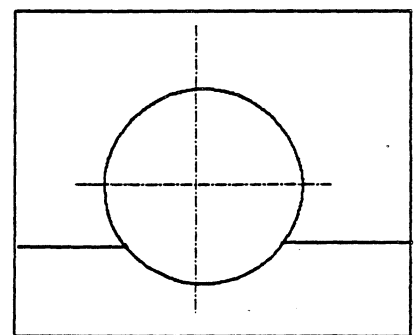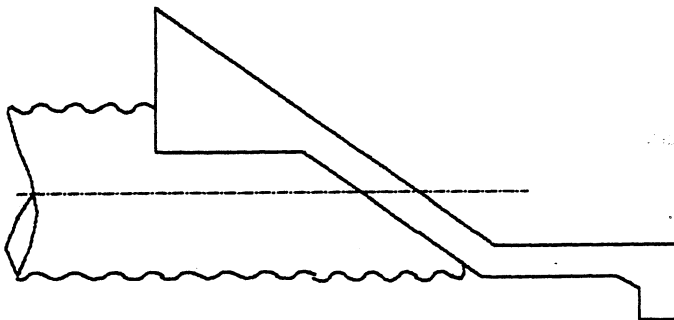
Figure 3.1   Types of headwalls described by agencies responding
             to survey.

Head walls are vertical concrete walls, perpendicular to the axis of the pipe, that extend above the top of square ended pipe.

Wing walls are similar to head walls but incorporate vertical walls on both sides at an angle to the to the axis of the pipes. The angled wing walls serve to direct flow into the pipe, avoid erosion or piping adjacent to the inlet, and add mass to resist uplift.

Slope collars may be either concrete or metal. The collars surround the culvert inlet, perpendicular to the pipe axis, and are parallel to soil slope of the embankment above the culvert.

Three agencies avoid the uplift problem by not using CMP and six others limit the maximum diameter of CMP. The maximum diameters range from 54 to 84 inches.

Anchor walls are used by 8 agencies, headwalls by 6, wing walls by 4, concrete slope collars by 5, and metal slope collars by 3. One agency uses anchor walls for CMP less than 48 inches in diameter and either slope collars or wing walls for pipe larger than 48 inches in diameter. A northern agency uses anchor walls on pipes 12 to 54 inches in diameter with the latter as the maximum diameter they will use. An agency from eastern United States uses wing walls on CMP between 36 and 72 inches diameter and headwalls on pipes 48 inches in diameter. The maximum diameter CMP that the eastern state uses is 72 inches. One north-central agency uses a system of longitudinal stiffeners.

3.4. Force Comparison of Various Restraints

In order to compare the various restraints, for each standard, the resisting force of the restraint was computed for a range of pipe diameters and with a constant cover depth of 2 feet. When the data are compared, it is apparent that the relationships between the resisting forces and pipe diameters can be classified as either linear or exponential shaped curves. The following graphs, Figs. 3.2 and 3.3, show the relationship between resisting force and pipe diameter according to various standards. In all cases but one, the end of the curve represents the maximum diameter CMP that the agency recommends. Also shown is the relationship resulting from the rational analysis of Austin et al (1990).

All of the agencies with standards having a linear relationship between force and diameter, shown in Fig 3.2, have standards that result in much lower forces than those calculated by Austin et al (1990). Agency 2 with the lowest forces in its standards is also the only one which had an uplift failure when restraint was used.

Agencies with standards that have an exponential relationship between resisting force and pipe diameter are shown in Fig. 3.3. Although the exponential curve of Austin et al (1990) was acknowledged to be extremely conservative; only one agency, with an exponential relationship between pipe diameter and resisting force, has standards with lower forces. The other three agencies have standards with resisting forces that are
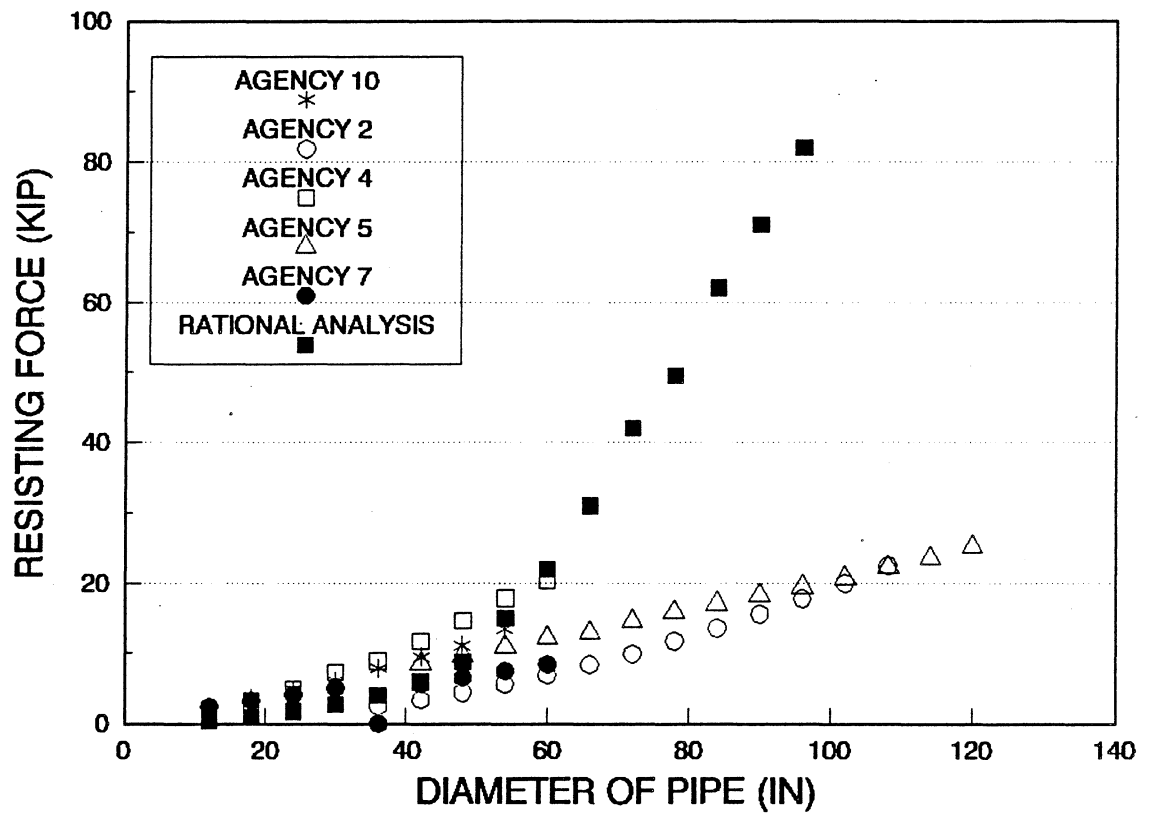
Figure 3.2 Relationship (Linear) between resisting force and pipe
diameter according to various standards.
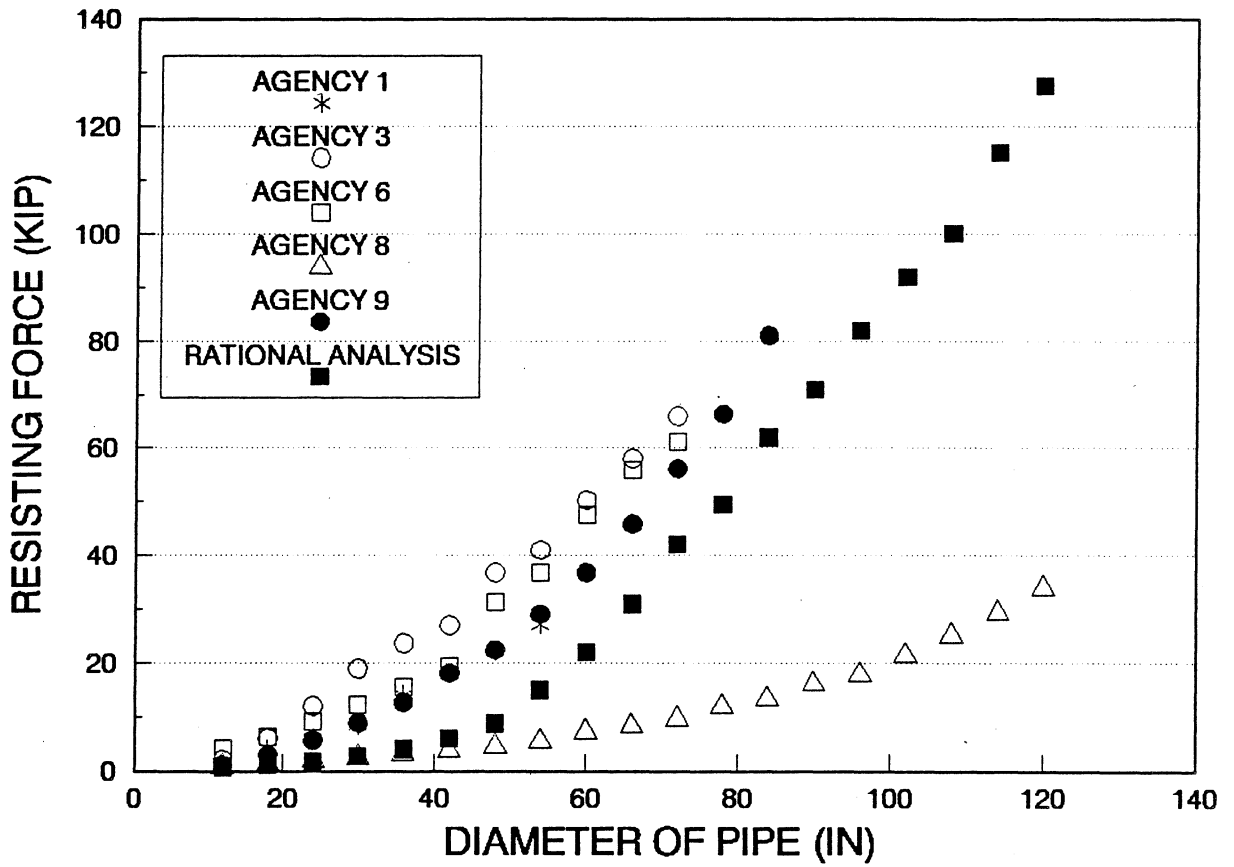
Figure 3.3 Relationship (Exponential) between resisting force and pipe diameter according to various standards.

equal or exceed those of Austin et al.

3.5 Conclusions from Survey of Agencies

In general, uplift failures of CMP throughout North America and Puerto Rico are fairly rare with only 17% of the agencies reporting failures within the last five years. Of those reporting failures, only one agency had used end restraint standards. Twenty six of 52 agencies have standards and three other agencies do not use CMP. Of those agencies that provided data to compare end restraint force as a function of CMP diameter, five have lower resisting forces than those computed by Austin et al (1990) and three have forces approximately equal or slightly greater. The large range in these standards and the continuation of uplift failures suggest that experimental work including the determination of pipe longitudinal stiffness and soil-pipe interaction is appropriate to develop a rational set of standards for end restraint.

4. TESTING

4.1. Overview of Testing Program

Because no longitudinal stiffness data for large diameter CMP are available in the literature, a program of flexural tests on larger diameter CMP was initiated. Three specimens, 4 feet, 6 feet, and 8 feet in diameter, were selected for testing. The specimens are identified as ISU1, ISU2, and ISU3 respectively and are described in Table 4.1.

4.2. Test Frame

In order to test each CMP in flexure, specimens were simply supported and distributed loads were applied in increments. As shown in plan view in Figure 4.1, independent frames support each end of the test specimen. A side view, an end view, and photograph of the test set-up are shown in Figures 4.2, 4.3, and 4.4, respectively.

Wire rope of 5/8 inch diameter suspended between columns of the frames provided end support for the CMP. The wire rope support permitted testing of CMP up to 9.5 feet in diameter with no modifications and allowed end rotation of the CMP. The CMP deflections were corrected for wire rope elongation.

The test frame was designed to resist the loads associated with the testing of the largest test specimen. The geometry of the wire ropes under load was determined so that rope tensions and corresponding loads on the frame could be calculated for each test specimen. The test frame was designed with sufficient stiffness to minimize column movements and limit rotation in the

Table 4.1 Flexural test specimens and instrumentation.

Parameter	Specimen		
	ISU1	ISU2	ISU3
Diameter (in.)	48	72	96
Corrugation style	3 x 1	3 x 1	3 x 1
Fabrication style	Helical welded seam	Helical welded seam	Helical welded seam
Nominal length (ft)	20	25	24
Effective length (in.)	236.5	293.5	286.0
Gage	12	14	14
Nominal uncoated thickness (in.)	0.1046	0.0747	0.0747
Weight (lb/ft)	50	75	100
Dial gage @ free end (Fig. 4.13)	Yes	No	No
Dial gage @ horizontally restrained end (Fig. 4.13)	Yes	Yes	Yes
DCDT's around circumference @ mid-span (Fig. 4.11)	Yes	Yes	Yes
Mid-span strains on compression side (Fig. 4.9)	Yes	Yes	Yes
Mid-span strains on tension side (Fig. 4.9)	Yes	Yes	Yes
Quarter-span strains on compression side (Fig. 4.10)	Yes	Yes	Yes
Quarter-span strains on tension side (Fig. 4.10)	DCDT (no strain gage)	Yes	Yes

Table 4.1 Continued.

Parameter	ISU1	ISU2	ISU3
Mid-span horizontal deflection (Fig. 4.12)	Yes	Yes	Yes-SL[1] No-F[2]
Mid-span vertical deflection (top) (Fig. A.1)	Yes	Yes	Yes
Mid-span vertical deflection (bottom) (Fig. A.1)	Yes	Yes	Yes
Quarter-span vertical deflections (bottom) (Fig. A.1)	Yes	Yes	Yes

[1] service load test

[2] failure test
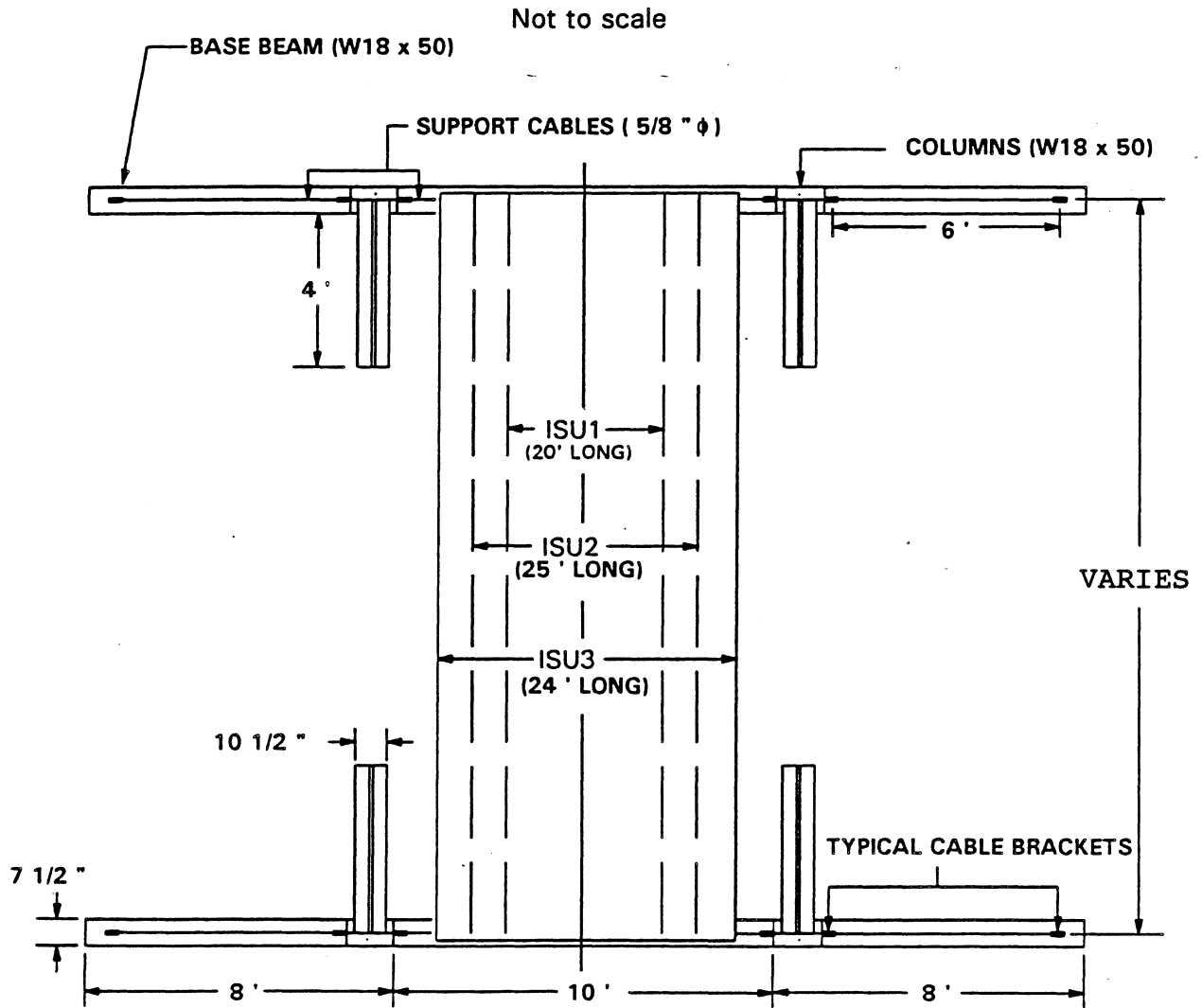
Figure 4.1 Plan view of load frames.
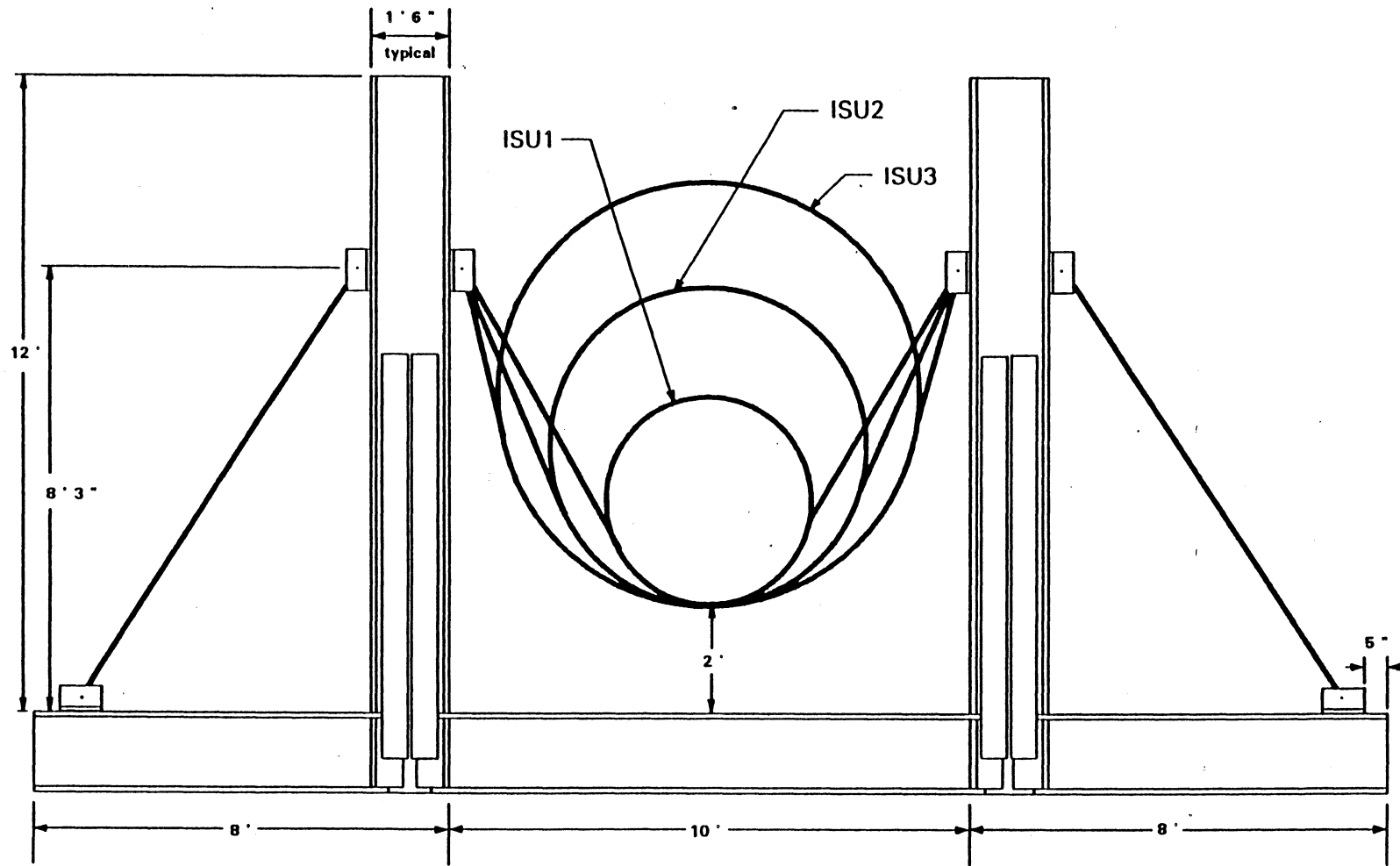
Figure 4.2 End view of typical load frame.

Not to scale

2 - 6 x 4 x 3/8 angles

ISU3

ISU2

ISU1

7'3"

2 - 5 x 5 x 3/8
angles

1 ' 6 "

W 18 x 50

4 '
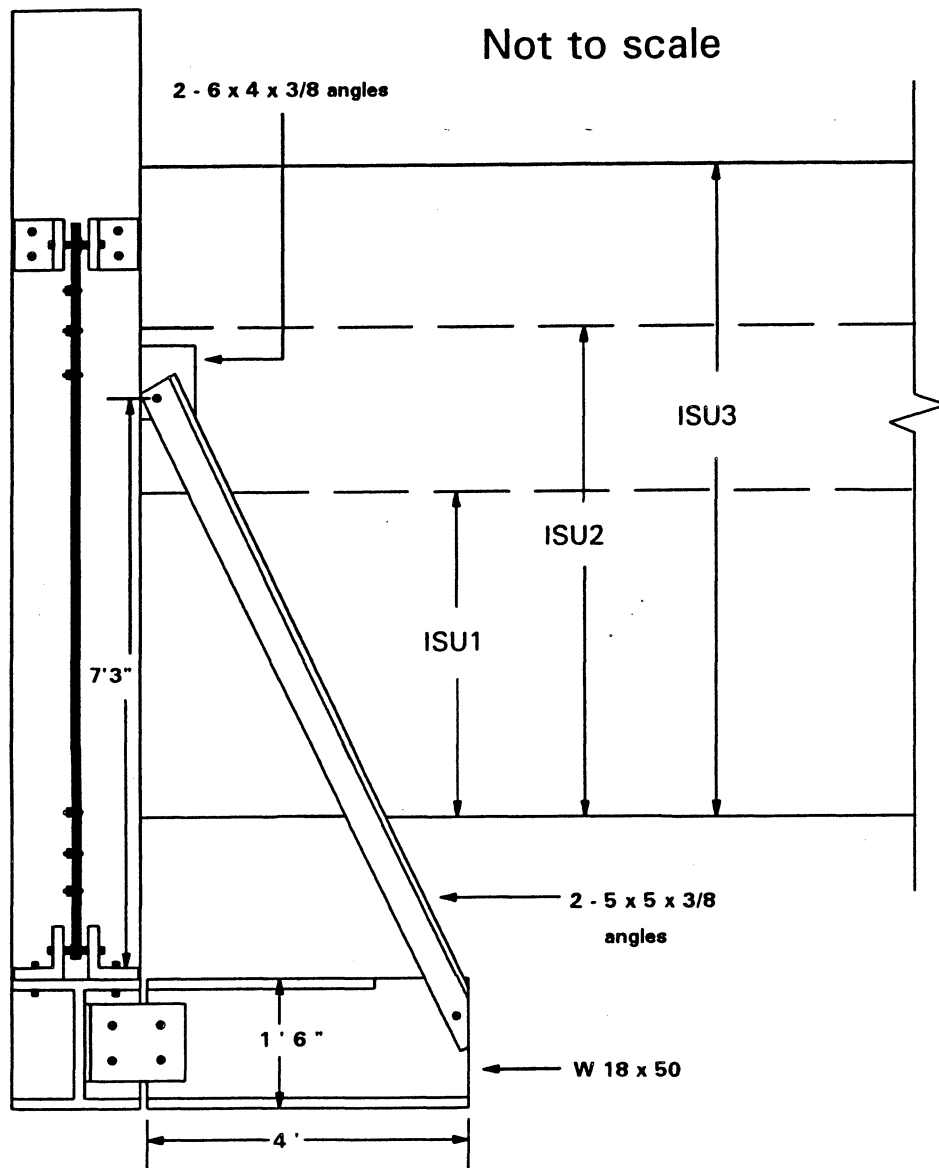
Figure 4.3   Side view of typical load frame.
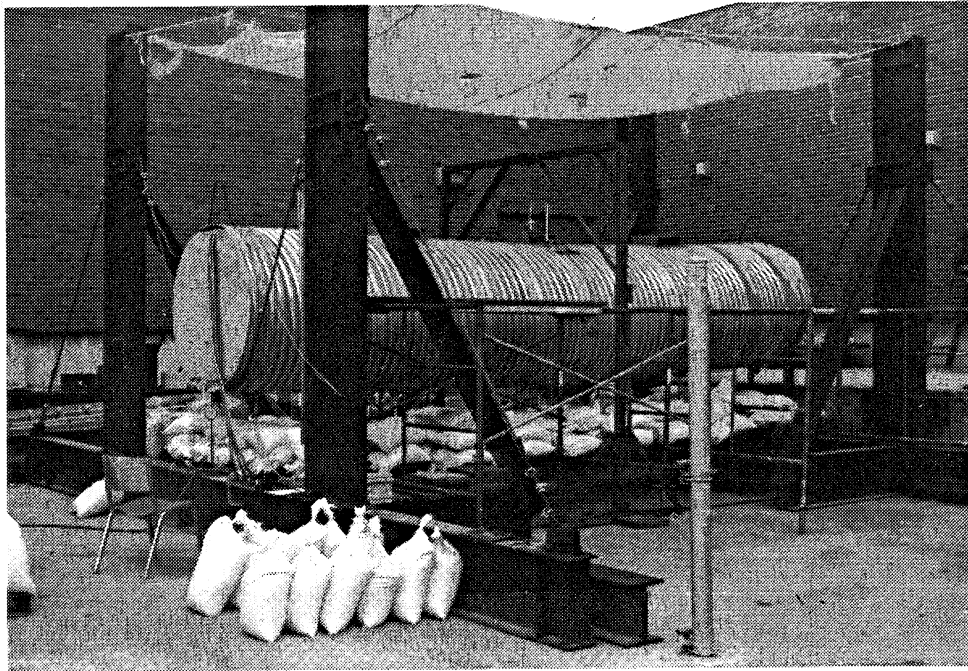
Figure 4.4 Photograph of load frame with ISU1 being tested.
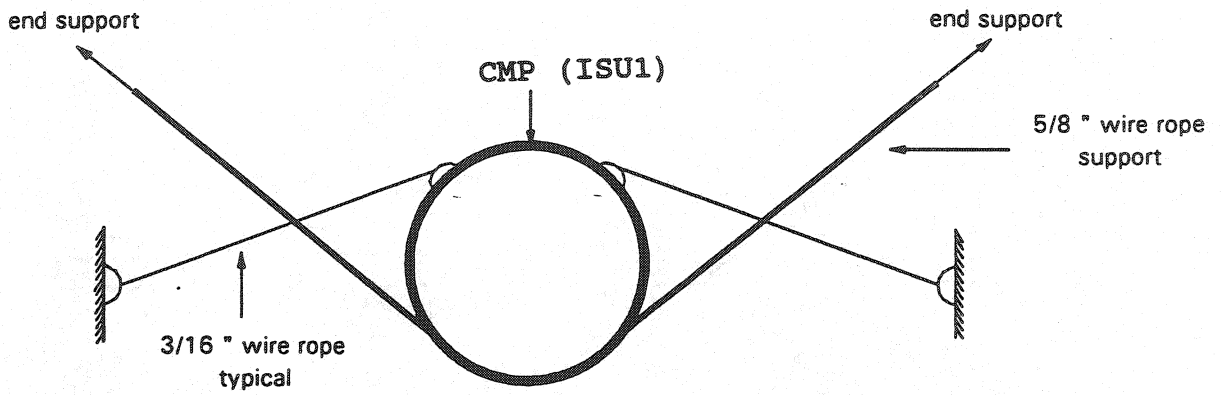
(a) restraint with tie-cables
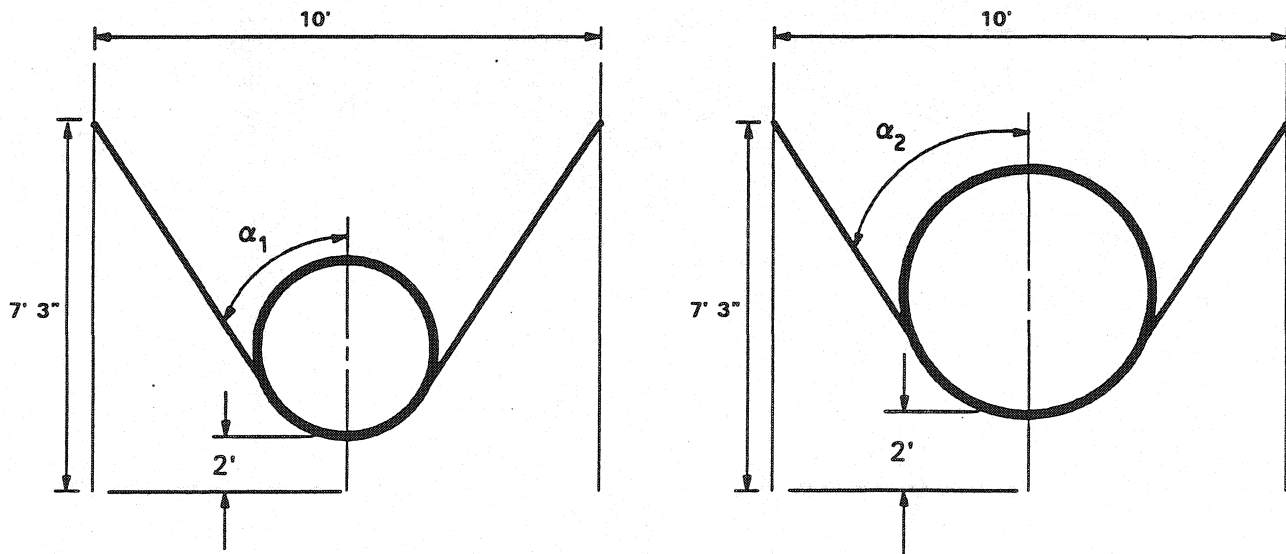
(b) inherent restraint due to upward angle of end support wire rope

Figure 4.5 CMP rotational restraint.
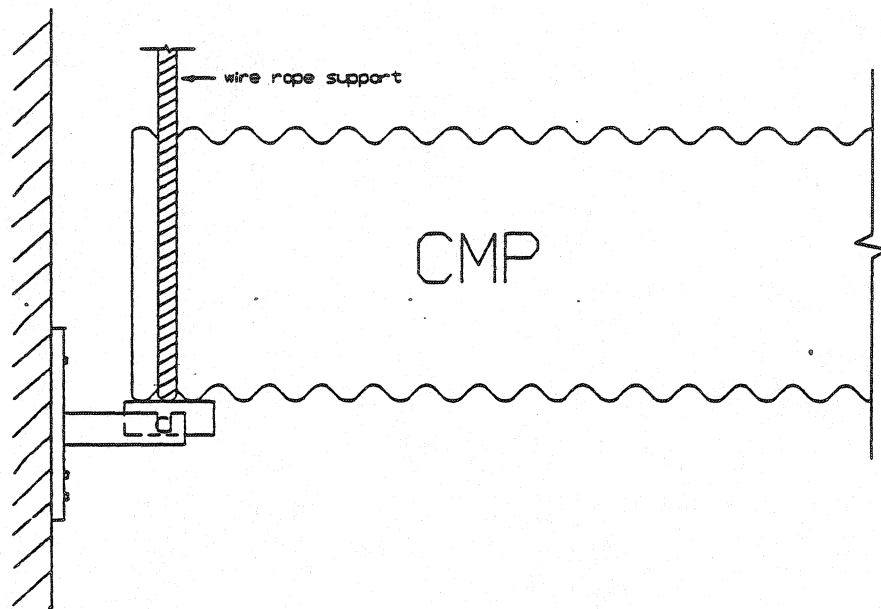
Figure 4.6   CMP longitudinal restraint.

Concrete

Steel
Reinforcement

Steel angle
3 x 3 x 3/16

Ties

6"
nominal
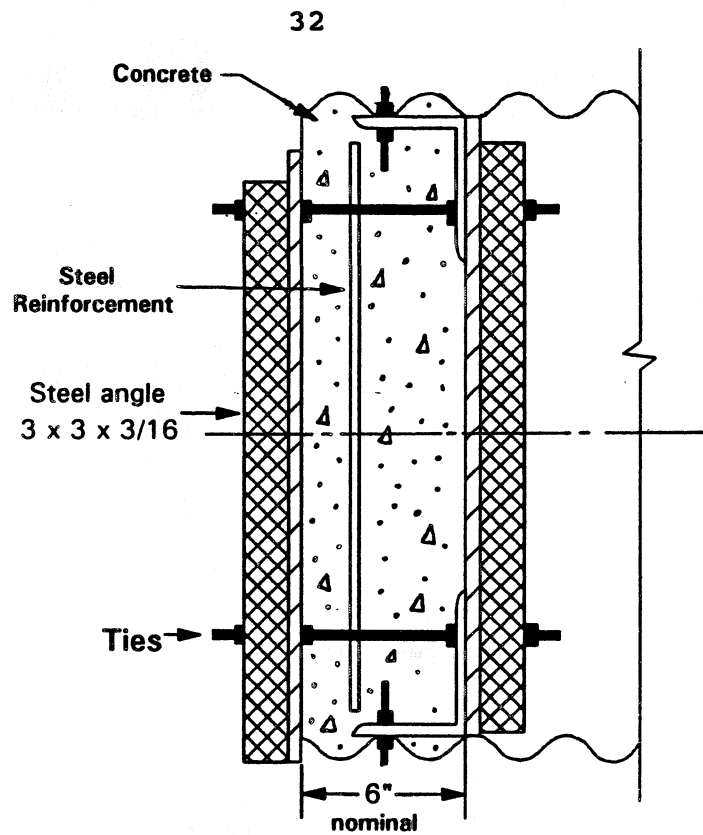
(a)   longitudinal section view through typical CMP diaphragm
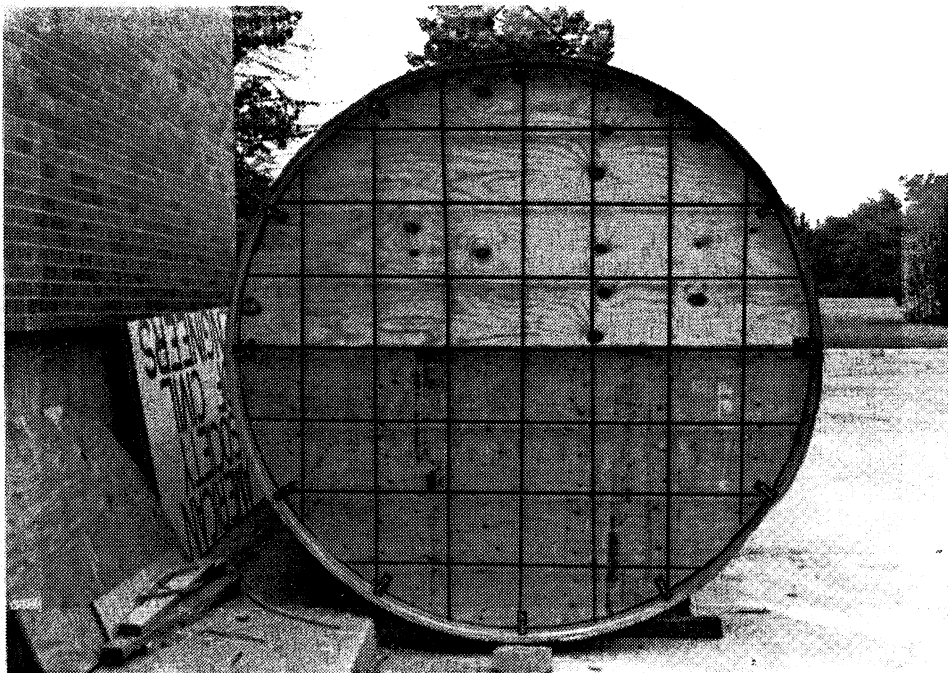
(b)   end view of typical CMP diaphragm showing steel
      reinforcement

Figure 4.7   CMP diaphragm details.
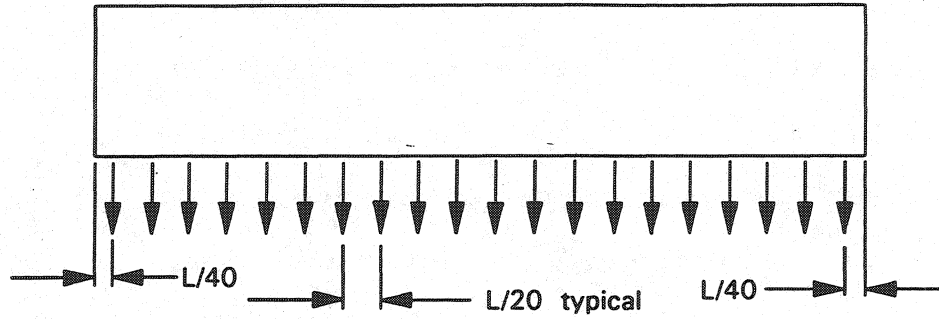
(a) longitudinal view of CMP specimen
with locations of "distributed" loads
suspended below specimen

uniform load on
top of CMP

L/40   L/20 typical   L/40

uniform load below CMP (only used for ISU1)
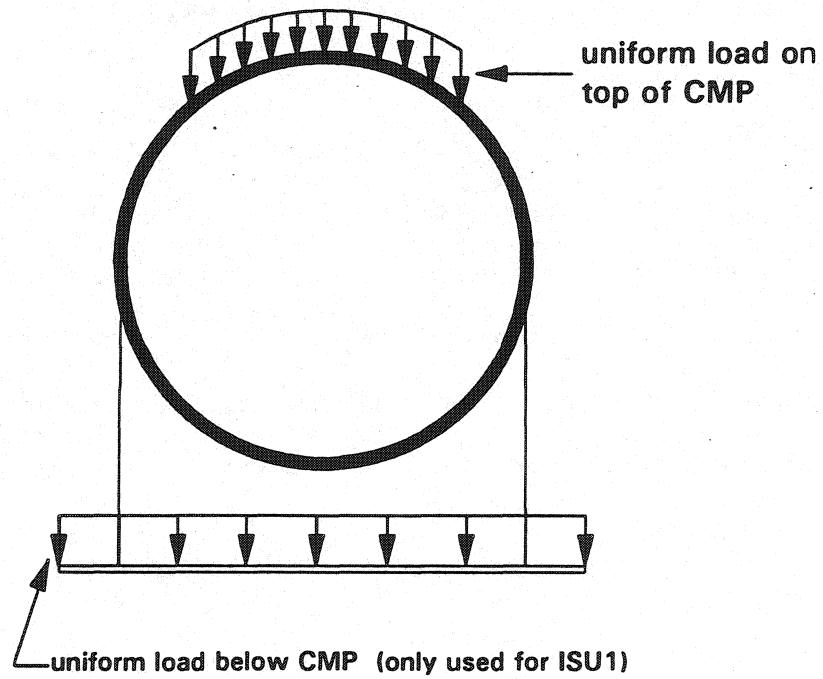
(b) transverse view of CMP specimen

Figure 4.8   Sand loading on CMP.

longitudinal direction during testing.

For the specimen 4 feet in diameter, it was necessary to provide restraint to prevent the CMP from rotating about its longitudinal axis if loading was placed slightly off center (see Figure 4.5a). For larger specimens, the possibility of rotation was limited as the angle of the wire rope end support decreased (i.e. in Figure 4.5b $\alpha_2 < \alpha_1$).

Horizontal restraint on one end of the CMP prevented longitudinal pipe movement as shown in Figure 4.6. These brackets, while limiting longitudinal movement, allowed end rotation of the CMP and elongation of the wire rope end supports.

4.3. CMP Diaphragms

Reinforced concrete diaphragms in both ends of the CMP specimens contained the water used as load inside of the pipes and also prevented potential distortion of the CMP cross section at the ends. A longitudinal section through the diaphragms in Figure 4.7a illustrates how the diaphragms are connected to the CMP. Reinforcement for the diaphragms is shown in Figure 4.7b.

4.4. Test Loading

Sandbags and water provided the loads on and in the pipes. The sandbags were used in the elastic range of each test and usually were stacked symmetrically about the centerline on the top of the CMP as shown in Figure 4.8. When testing Specimen ISU1 to failure, sandbags were also suspended from the CMP on platforms supported by 3/16 inch wire rope as shown in Figure 4.8b. Water load inside the pipes was combined with sand load to

provide enough load to collapse the specimens. As the CMP
deflected vertically, the water load was no longer uniform along
the CMP length therefore moments rather than loads are used to
characterize the response of the pipes.

The testing program included a service load test and a
failure load test for each specimen. Service loads were assumed
to induce a moment in the CMP which resulted only in elastic
deformations and included both loading and unloading. Loading in
the service load tests was limited so that the maximum was
applied in the elastic range, approximately 1/2 of the ultimate
moment capacity of the CMP. The ultimate moment capacity was
estimated using limited information provided by a manufacturer of
CMP. In the failure load tests, the CMP was loaded until a
corrugation collapsed on the compression side of the CMP. It was
assumed that data from the elastic range of the failure test
would replicate the data from the service load test. Tables 4.2
through 4.7 present loadings and longitudinal mid-span moments on
the three specimens. Service load tests are referred to as
ISU1SL, ISU2SL, and ISU3SL; similarly, failure load tests are
referred to as ISU1F, ISU2F, and ISU3F.

4.5. Test Instrumentation

Test specimens were instrumented with six types of
instrumentation including: electrical resistance strain gages,
direct current displacement transducers (DCDT), vertical
deflection gages, horizontal deflection gages, dial gages to
monitor wire rope elongation, and a water level monitor.

Table 4.2 Test loading - ISU1SL.

Load point	Uniform distributed load (lb/ft)	Non-uniform distributed load (lb/ft)	Mid-span moment (k-ft)
1	0	0	2.43
2	70	"	5.83
3	140	"	9.24
4	210	"	12.6
5	315	"	17.8
6	"	56	22.6
7	"	106	25.5
8	"	158	28.4
9	"	214	31.6
10	"	269	34.7
11	"	320	37.6
12	"	371	40.5
13	"	423	43.4
14	"	480	46.5
15	"	536	49.5
16	"	584	52.1

Table 4.3 Test loading – ISU1F.

Load point	Uniform distributed load (lb/ft)	Non-uniform distributed load (lb/ft)	Mid-span moment (k-ft)
1	0	0	5.83
2	175	"	11.0
3	350	"	19.5
4	467	"	25.2
5	642	"	33.7
6	712	"	37.1
7	782	"	40.5
8	852	"	43.9
9	957	"	49.0
10	1062	"	54.1
11	1062	56	57.0
12	Non-uniform *	56	30.9
13	782	299	67.5

* Irregular arrangement of sand load on specimen due to load failure as discussed in section 4.1

Table 4.4   Test loading - ISU2SL.

Load point	Uniform distributed load (lb/ft)	Non-uniform distributed load (lb/ft)	Mid-span moment (k-ft)
1	0	0	5.61
2	"	54	10.5
3	"	107	15.4
4	"	165	20.7
5	"	223	27.5
6	"	280	33.2
7	"	332	37.3

Table 4.5   Test loading - ISU2F.

Load point	Uniform distributed load (lb/ft)	Non-uniform distributed load (lb/ft)	Mid-span moment (k-ft)
1	0	0	5.61
2	"	107	15.8
3	"	165	21.3
4	"	223	28.1
5	"	273	32.9
6	"	332	37.4
7	"	386	43.0
8	"	442	49.3
9	"	493	56.2
10	"	552	66.1
11	"	582	72

Table 4.6 Test loading - ISU3SL.

Load point	Uniform distributed load (lb/ft)	Non-uniform distributed load (lb/ft)	Mid-span moment (k-ft)
1	0	0	7.81
2	"	62	12.2
3	"	125	17.1
4	"	186	21.9
5	"	247	26.9
6	"	313	32.3
7	"	375	37.4
8	"	440	42.7
9	"	499	47.7
10	"	560	52.7
11	"	622	58.0
12	"	686	63.4
13	"	752	68.9
14	"	809	73.8
15	"	876	79.7
16	"	935	84.9
17	"	994	90.1
18	"	1064	96.7
19	"	1125	102
20	"	1186	109

Table 4.7   Test loading - ISU3F.

Load point	Uniform distributed load (lb/ft)	Non-uniform distributed load (lb/ft)	Mid-span moment (k-ft)
1	0	0	7.81
2	70	"	12.1
3	130	"	16.3
4	190	"	20.6
5	250	"	24.9

Strain gages were attached to the CMP surface and coated with polyurethane as a moisture barrier. These 120 ohm gages with three-wire leads were wired in a quarter-bridge configuration. Strain gages are on the CMP centerline as shown in Figure 4.9; a diagram of a typical corrugation (both on the tension and compression sides of the pipe) with strain gage locations is shown in Figure 4.9. Strain gages were also mounted, as shown in Figure 4.10, at the quarter-point locations on the CMP to determine if the pipe was bending symmetrically.

DCDT's were used to measure the movements between the corrugation peaks and were oriented around the circumference of the pipe at the longitudinal mid-point as shown in Figure 4.11

Vertical deflections were determined by reading CMP elevations on engineering scales suspended from the bottom of the CMP at the quarter points and at the mid-span as well as a scale attached to the top of the CMP at the mid-span. The scales were read with surveying transits. Engineering scales were used because large deflections were expected. Deflections as large as 21 inches could be measured with reasonable accuracy as the scales were accurate to the nearest 0.005 of a foot. Vertical deflections were used to calculate the flexural stiffness of the CMP, to quantify the deflected shape of the CMP, and to determine changes in the CMP vertical diameter.

The deflected shape was used to account for the non-uniform depth of water along the length of the CMP as discussed in the Section 4.4. Variations in the water depth along the CMP were
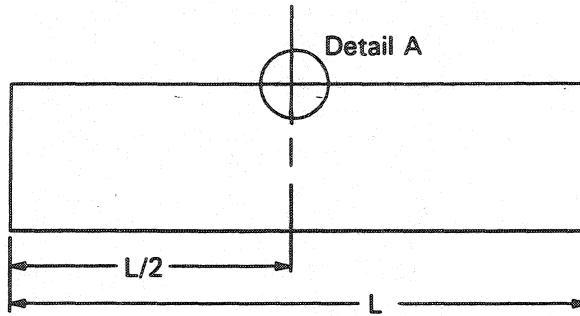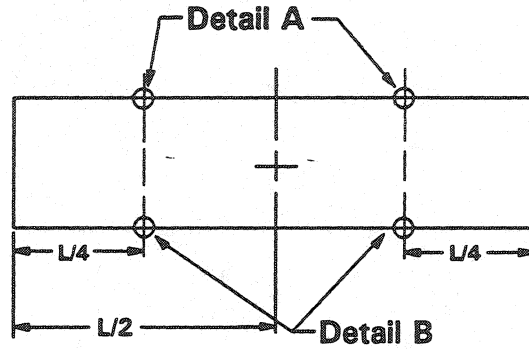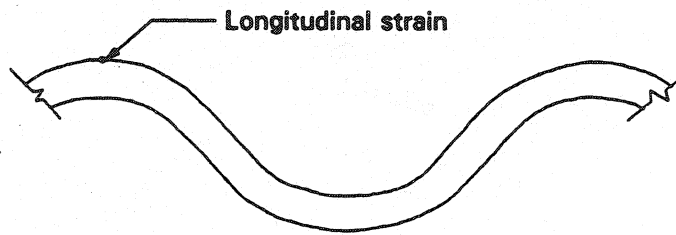
(a) CMP specimen
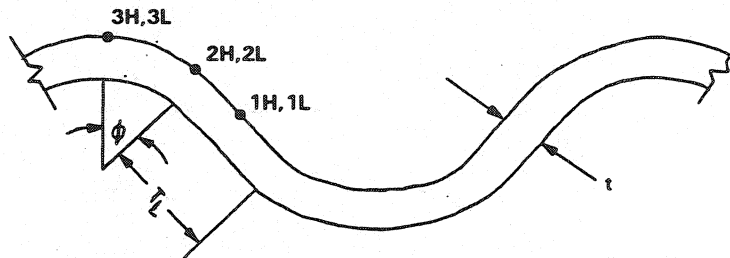
Gauge	Location	Orientation
1H	Inflection Point	Hoop
1L	Inflection Point	Longitudinal
2H	Tangent Point	Hoop
2L	Tangent Point	Longitudinal
3H	Crest	Hoop
3L	Crest	Longitudinal

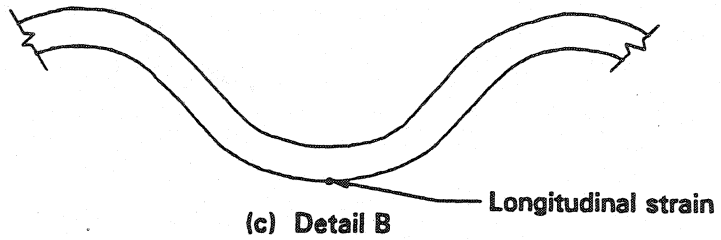(b) Detail A; strain gages are at mid-span

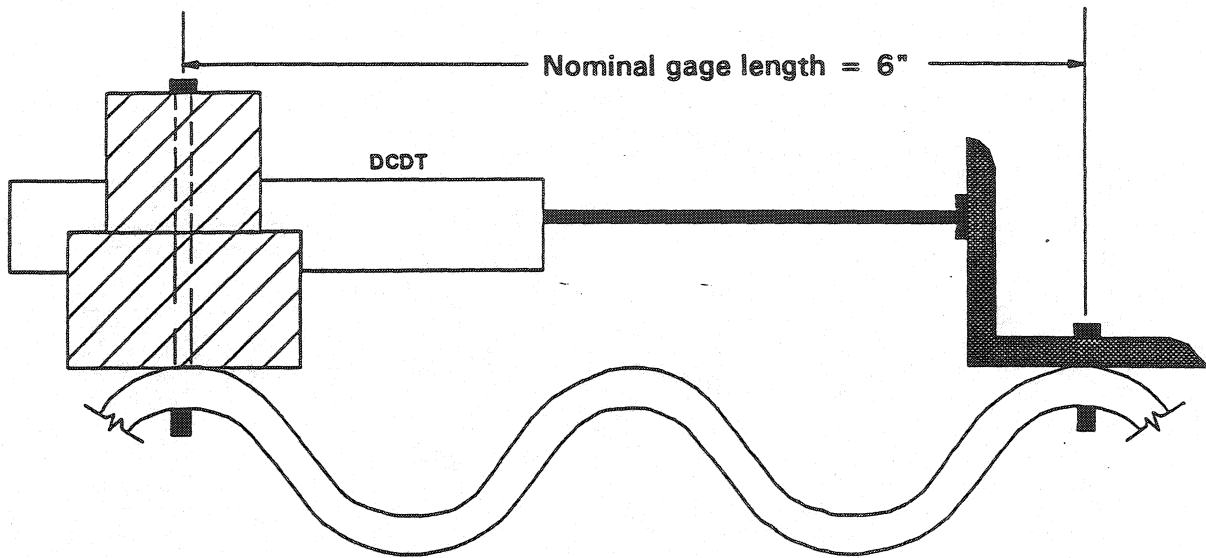Figure 4.9 Typical location of strain gages at mid-span.
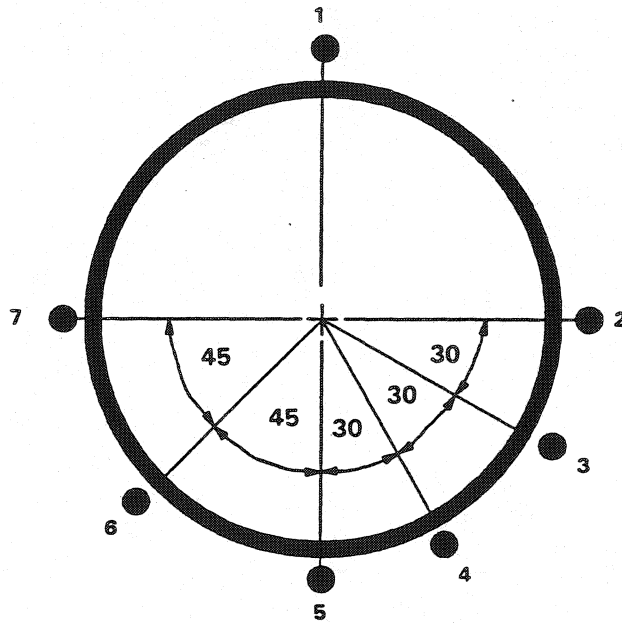
(a) CMP specimen

(b) Detail A

(c) Detail B

Figure 4.10 Typical location of strain gages at quarter-spans.

Nominal gage length = 6"

DCDT

(a)   attachment of DCDT to corrugation

1

7

45

30

30

45

30

2

3

4

5

6

(b)   locations of DCDT installations around the transverse section
       view

Figure 4.11   Installation of DCDT's at CMP mid-span.

used to calculate the moment caused by the non-uniform load. Vertical deflections of the top and bottom of the CMP were subtracted to determine changes in diameter of the CMP at the centerline.

A steel rod and DCDT were placed horizontally between adjacent walls of each test specimen to measure changes in the horizontal CMP diameter (see Figure 4.12). This allows the measuring system to move with the CMP during testing.

Dial gages were used to measure vertical deflection due to wire rope elongation at the end support locations as shown in Figure 4.13. Vertical deflections were needed to determine actual CMP vertical deflection as noted in Section 4.2.

To determine the depth of water in the CMP at any time, three flexible tubes were attached to the bottom of the test specimens and positioned vertically on a calibrated board. The water level in the tubes was the same as the water level in the CMP. Although this system was simple, it was quite accurate. The only problem occurred with test Specimen ISU2 which deflected to such an extent that the top of the CMP at the middle came in contact with the water surface during the failure test. The CMP then became pressurized and the water depth readings were not accurate.

Water depth data and vertical deflection data were recorded manually after each load increment. Data from all strain gages and DCDT's were recorded with a Hewlett-Packard data acquisition system (DAS).
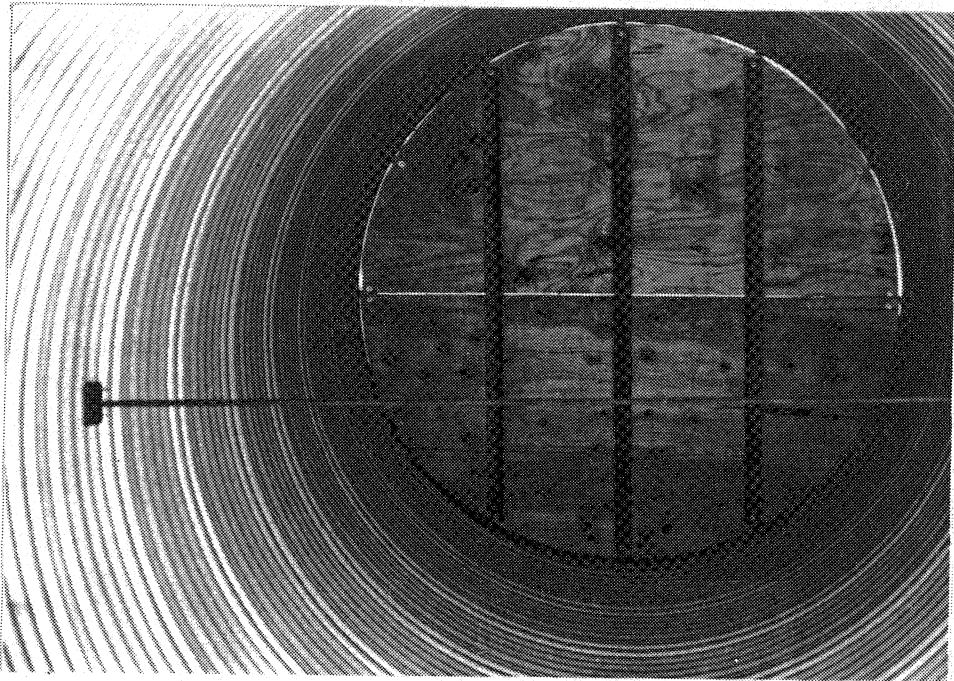
Figure 4.12 Interior view of diaphragm form and rod used to
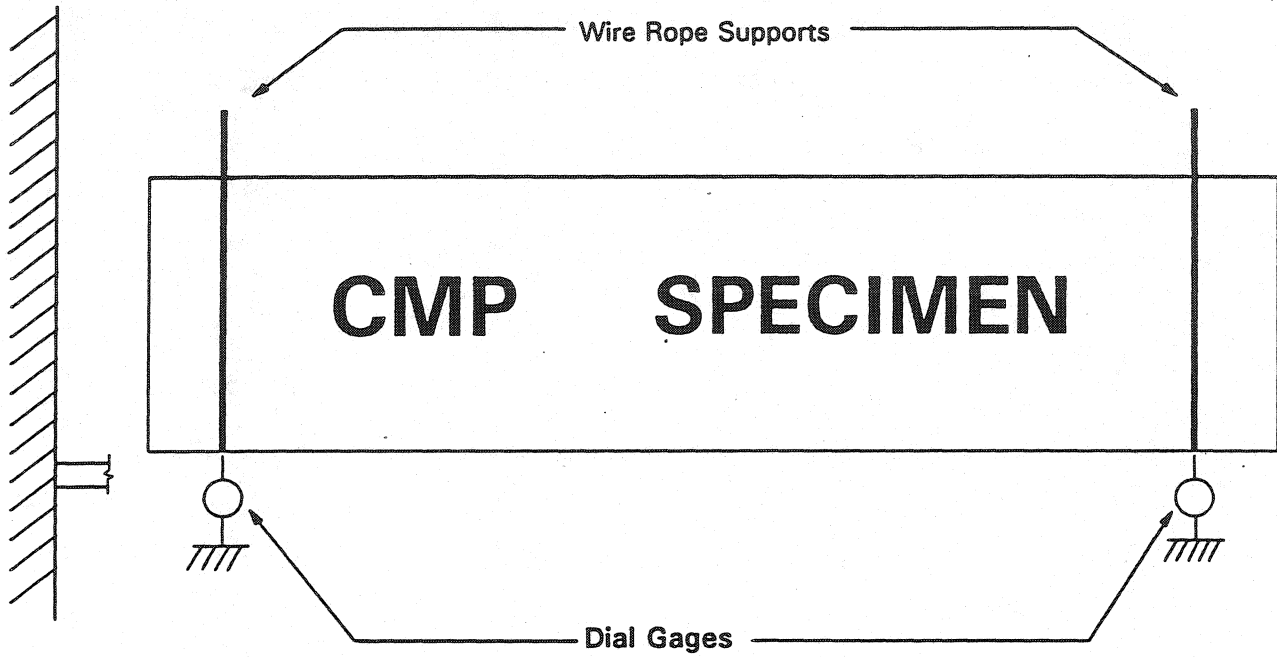measure relative wall movement.

Figure 4.13   Dial gages to measure CMP deflection due to cable
elongation.

4.6. Uniaxial Tensile Tests

Two CMP wall sections were removed from Specimen ISU3 and tested in uniaxial tension according to ASTM standard E-8 (ASTM, 1991). Because of the curvature of the specimens, strain gages were utilized to measure biaxial strains on both sides of the specimens. The strains from both sides were averaged to account for the bending that occurred as the specimens straightened during the tension test.